Hydrol. Earth Syst. Sci. Discuss., 10, 11983–12026, 2013
www.hydrol-earth-syst-sci-discuss.net/10/11983/2013/
doi:10.5194/hessd-10-11983-2013

Hydrology and
Earth System
Sciences
Discussions
Open Access

Senstitivity of water balance components to environmental changes in a mountainous watershed: uncertainty assessment based on models comparison

E. Morán-Tejeda[1], J. Zabalza[2], K. Rahman[1], A. Gago-Silva[1], J. I. López-Moreno[2], S. Vicente-Serrano[2], A. Lehmann[1], C. L. Tague[3], and M. Beniston[1]

[1]Institute for Environmental Studies, University of Geneva, Switzerland
[2]Pyrenean Institute of Ecology, CSIC, Spain
[3]Bren School of Environmental Science and Management, University of California, USA

Received: 6 September 2013 – Accepted: 21 September 2013 – Published: 1 October 2013

Correspondence to: E. Morán-Tejeda (enriquemoran@gmail.com)

Published by Copernicus Publications on behalf of the European Geosciences Union.

Abstract

This paper evaluates the response of stream flow and other components of the water balance to changes in climate and land-use in a Pyrenean watershed. It further provides a measure of uncertainty in water resources forecasts by comparing the performance of two hydrological models: Soil and Water Assessment Tool (SWAT) and Regional Hydro-Ecological Simulation System (RHESSys). Regional Climate Model outputs for the 2021–2050 time-frame, and hypothetical (but plausible) land-use scenarios considering re-vegetation and wildfire processes were used as inputs to the models. Results indicate an overall decrease in river flows when the scenarios are considered, except for the post-fire vegetation scenario, in which stream flows are simulated to increase. However the magnitude of these projections varies between the two models used, as SWAT tends to produce larger hydrological changes under climate change scenarios, and RHESSys shows more sensitivity to changes in land-cover. The final prediction will therefore depend largely on the combination of the land-use and climate scenarios, and on the model utilized.

1 Introduction

Water availability and water resources management are key aspects of the environment and socio-economic systems of the Mediterranean region (García-Ruiz et al., 2011). The climate and consequently the river regimes display high variability both on inter and intra-annual time scales. The high dependence of economies on summer tourism or on intensive irrigated agriculture implies that higher demand of water coincides with the timing of the least availability of water. Therefore it is often necessary to use hydraulic infrastructures and complex management schemes that enable to respond to the water needs of different users (López-Moreno et al., 2008). In these environments mountains play an essential role for water availability because they are the source of more than half of the annual runoff (Viviroli and Weingartner, 2004).

Mountains store water in both liquid and solid phases and release runoff to streams on a permanent basis, ensuring fresh water availability even during the dry season.

The social and demographic changes related to economic development during the last decades have had contrasted impacts in mountains and downstream areas. In Mediterranean countries, such Spain, mountains have suffered an intense depopulation and abandonment of traditional activities, and downstream areas have experienced the opposite trend, with an increase of population and industrial activities. Numerous studies have demonstrated that the decrease of human pressure on mountains resulting from the abandonment of rural activities have resulted in increasing vegetation cover, due to natural re-vegetation of slopes, including the substitution of croplands and rangelands by shrubs or even an expansion of forests (Lasanta-Martínez et al., 2005; Vicente-Serrano et al., 2004; Poyatos et al., 2003). The abandonment of lands is related to the increase of wildfires in the Mediterranean region. Specifically in Spain wildfires have experienced a significant increase since the 70s due to climate and land-use changes as demonstrated by Pausas (2004). Wildfires are responsible for landscape degradation and they can also modify their hydrological dynamics, due to their effect on vegetation and soil properties (Shakesby, 2011; Mayor et al., 2007). Together with changes in land-cover, systematic changes in the climatic variables involved in the water cycle (e.g. precipitation, temperature, evapotranspiration) may induce notable alterations in the runoff released by mountains. Hydrological processes in mountains are highly sensitive to changes in climate, as both precipitation and temperature can experience abrupt changes over short distances due to the altitudinal gradients and differing exposures to radiation and winds (Beniston, 2005). Increasing temperatures affect evapotranspiration rates and, in snow-dominated mountain regions can have a large impact on the amount of accumulated snow and in the timing of accumulation and melting, with subsequent alteration of hydrological regimes (López-Moreno and García-Ruiz, 2004; Tague and Peng, 2013).

A comprehensive understanding of the processes that govern the water balance in mountains is crucial to ensure suitable management of water resources in downstream areas. For this headwater areas present an advantage with respect to floodplain areas, as a result of the lack of disturbance by reservoirs or artificial channels for water diversion. However, climatic and hydrological monitoring in mountains is difficult, due to the high costs and human effort for the installation and maintenance of monitoring stations. Therefore the density of stations in the headwater areas is much lower than that of the downstream areas. In order to overcome this problem, hydrological models can be used; not only do they represent a successful tool to overcome the lack of observational data, they also allow predicting the possible response of hydrological parameters to changes in input conditions. Whereas simplistic conceptual models such as rainfall-runoff models can be useful for climate impacts studies in homogeneous environments, more complex physically-based models are required when spatial heterogeneities in the watersheds are to be investigated (Krysanova and Arnold, 2008) The "process-based" hydrological models allow reproducing, through empirical equations, the physical processes of the watersheds, and they yield hydrological variables including runoff, evapotranspiration, groundwater recharge or snowpack water content, in a distributed fashion and at different spatial and temporal scales. These models therefore constitute valuable tools for water management and decision making in the context of environmental change (Borah and Bera, 2004).

However, it is widely recognized that hydrological modeling involves a wide range of uncertainties and it is the responsibility of the model user to acknowledge them (Pappenberger and Beven, 2006). These include uncertainties related to the input data, those pertaining to the complexity in the structure of the model, those linked to the calibration of an excessive number of parameters, or related to scale (see sources of uncertainty in: Wagener and Gupta, 2005). Complex statistical algorithms have been developed by modelers in order to deal with uncertainties related with calibration procedures, e.g.: GLUE (Beven and Binley, 1992), ParaSol (Van Griensven and Meixner, 2006), or SUFI-2 (Abbaspour et al., 2004), but even so, the internal structure or complexity of the model itself can represent a problem when interpreting results (Butts et al., 2004; Krysanova and Arnold, 2008). The hypothesis underlying the present work is that a major source of uncertainty can be linked to the selection of the model used for hydrological forecasting.

The objective of this paper is to assess the hydrological sensitivity of a mountainous watershed to changes in land-cover and climate by comparing the performance of two process-based hydrological models of contrasted conception and applicability: the Regional Hydro-Ecologic Simulation System (RHESSys), and the Soil Water Assessment Tool (SWAT) Results of this comparison provide an assessment of uncertainty in hydrologic model due to model selection in the context of estimating land-cover and climate change for mountain headwaters. The selected catchment has a crucial resource management importance as it feeds the Yesa reservoir, which provides water for irrigated croplands located in the semi-arid region of the Ebro basin.

2 Study area

The upper Aragón catchment is located in the Central Pyrenees (northern Spain) and it is drained by the Aragón River and its tributaries (Fig. 1). It has a spatial extent of almost 1500 km^2, and a mean altitude of 1170 m. The lower point of the catchment (492 m) coincides with the hydrological station at the mouth of the Yesa reservoir; therefore the reservoir is excluded from the study area, in order to focus on streamflows following a natural unmanaged regime. The Aragón catchment exhibits relatively moist climatic conditions, with precipitation ranging from 750 mm yr^{-1} in the valley bottom, up to 1600 mm yr^{-1} in the highest and northernmost parts of the catchment. The mean annual temperature at the station of Canfranc (1115 m) is ≈ 8 °C, and lower values are registered in the highest parts of the basin (> 2600 m), favoring the consolidation of a snowpack during the winter season. Outside the limits of the catchment, the Yesa reservoir collects the flows from the Aragón river during the period of high flows (winter-spring) and provides water during summer to the irrigated croplands located in the dryer areas downstream.

The Aragón River, whose catchment can be considered representative of many other Pyrenean catchments, is a tributary of the Ebro river, one of the largest rivers in Spain. The Ebro basin is characterized by semi-arid conditions in the valley bottom, with low precipitation totals ($\approx 300\,\mathrm{mm\,yr^{-1}}$) and high rates of potential evapotranspiration ($\approx 1200\,\mathrm{mm\,yr^{-1}}$); however the river banks are occupied by irrigated croplands throughout the entire valley, as this is one of the most productive irrigated areas of northern Spain. Therefore, the fresh water released within the Pyrenees is of crucial importance for the economic development of the region, where highly populated and industrial cities such as Zaragoza or Lleida are located.

3 Material and methods

In this section the basic characteristics of the models used, as well as the necessary input data for model building, and the calibration procedures are described.

3.1 Models description

The selection of RHESSys and SWAT models for this study was based on different criteria including: the need of process-based distributed models in order to compare the effects of spatially distributed processes of change (land-use, climate change) at different spatial scales and over different components of the water balance; the need of two models of differing conception and purpose but with similar spatial partitioning, input requirements and hydrological output to make possible the comparison of results

The Regional Hydro-Ecological Simulation System (RHESSys) was designed to simulate integrated water, carbon and nutrient cycling and transport over complex terrain at small to medium scales (Tague and Band, 2004) Basins are subdivided into landscape units following a hierarchical classification, which enables modeling at various scales. At the finest scale patches are typically defined by areas on the order of $\mathrm{m^2}$, while basins (order of $\mathrm{km^2}$) define the largest scale. Various hydro-ecological processes are simulated including vertical energy and associated moisture fluxes (interception, infiltration, transpiration, evapotranspiration from littler and soil stores, subsurface drainage and groundwater recharge), and lateral moisture fluxes between spatial units based on topography and soil characteristics (Tague and Band, 2004).

The Soil and Water Assessment Tool (SWAT, Arnold et al., 1998) subdivides the watershed into sub-basins connected with the river network, and each sub-basin is divided into small and independent units called hydrological response units (HRUs). Each HRU represent a unique combination of land use, soil and slope. HRUs are non-spatially distributed assuming there is no interaction and dependency (Neitsch et al., 2005). SWAT has been successfully applied worldwide for solving various environmental issues for water quality and quantity studies (see review in: Gassman et al., 2007) SWAT simulates energy, hydrology, soil temperature, mass transport and land management at subbasin and HRU level.

The two models differ in the basic equations governing water partitioning and runoff generation, and this can be therefore the cause of possible differences in the results obtained from the analyses. Here we describe briefly the equations responsible for snowmelt, evapotranspiration, and surface runoff processes, in each model. The interested reader can find further details in the theoretical documentation manuals for SWAT (Neitsch et al., 2005) and RHESSys (Tague and Band, 2004).

3.1.1 Snowmelt

For RHESSys, snowmelt (q_{melt}) is computed based on a quasi-energy budget model that sums up the melting from radiation (M_{rad}), sensible and latent heat fluxes (M_T) and advection (M_v) (from rain on snow) on a daily basis:

$$q_{\text{melt}} = M_{\text{rad}} + M_T + M_v, \tag{1}$$

where melt from temperature and advection occurs only when the snowpack is mature. The calculations for each component of the Eq. (1) are described in detail in the aforementioned manual.

In SWAT snowmelt is based on a temperature-index model, and computed as following:

$$\mathrm{SNO_{mlt}} = b_{\mathrm{mlt}}\mathrm{sno_{cov}}\left[\frac{T_{\mathrm{snow}} + T_{\mathrm{mx}}}{2} - T_{\mathrm{mlt}}\right] \tag{2}$$

where $\mathrm{SNO_{mlt}}$ is the amount of snow melt in a given day (mm), b_{mlt} is the melt factor for the day ($\mathrm{mm\,d^{-1}\,{}^{\circ}C^{-1}}$), $\mathrm{sno_{cov}}$ is the fraction of the HRU area covered by snow, T_{snow} is the snowpack temperature of the given day (°C), T_{mx} is the maximum air temperature of the day (°C) and T_{mlt} is the base temperature above which snow melt is allowed.

3.1.2 Evapotranspiration

Evapotranspiration includes all processes by which water at the earth's surface returns to the atmosphere as water vapor. It includes evaporation from the soil and plant canopy, transpiration by plants and sublimation.

In RHESSys evapotranspiration is calculated using the standard Penman–Monteith (Monteith, 1965) equation:

$$\mathrm{ET}_o = \frac{\Delta\,(R_{\mathrm{n}} - G) + \rho_{\mathrm{a}} c_p(\delta_e) g_{\mathrm{a}}}{(\Delta + \gamma(1 + g_{\mathrm{a}}/g_{\mathrm{s}}))l_{\mathrm{v}}} \tag{3}$$

where ET_o is the water volume evapotranspired ($\mathrm{mm\,day^{-1}}$), Δ is the rate of change of saturation specific humidity with air temperature ($\mathrm{KPa\,{}^{\circ}C^{-1}}$), R_{n} is the net irradiance ($\mathrm{MJ\,m^{-2}\,day^{-1}}$), G is the heat flux density to the ground ($\mathrm{MJ\,m^{-2}\,day^{-1}}$) ρ_{a} is the dry air density ($\mathrm{kg\,m^{-3}}$), c_p is the specific heat at constant pressure ($\mathrm{MJ\,Kg^{-1}\,{}^{\circ}C^{-1}}$), δ_e is the vapor pressure deficit or relative humidity (Pa), g_{a} is the conductivity of air ($\mathrm{m\,s^{-1}}$), γ is the psychrometric constant ($\mathrm{Pa\,K^{-1}}$), g_{s} is the surface conductance ($\mathrm{m\,s^{-1}}$) and l_{v} is the volumetric latent heat of vaporization ($\mathrm{MJ\,m^{-3}}$). For soil and litter evaporation, g_{s} varies as a function of moisture content and texture. For transpiration, stomatal conductance is used for surface conductance and computed using a Jarvis multiplicative model (Jarvis, 1976), accounting for radiation, vapor pressure deficit, rooting zone soil moisture, CO_2, and temperature controls. We compute transpiration separately for sunlit and shaded leaves and scale these by respective sunlit and shaded leaf area based on Chen et al. (1999). Leaf-scale transpiration is then scaled to canopy-transpiration by integrating over the leaf area index.

In SWAT, for modeling actual evapotranspiration (ET), the model first need to estimate the potential evapotranspiration (ETP), which is the rate of evapotranspiration that would occur in conditions of unlimited availability of water for plants. The user can choose amongst different methods for ETP calculation, including the Penman–Monteith equation. However, when using this method for SWAT, results, both in real evapotranspiration (ET) and water yield were completely out of bounds, therefore we decided to use the Hargreaves method (Hargreaves and Samani, 1985), which calculates ETP as follows:

$$E_0 = \frac{0.0023 H_0 (T_{mx} - T_{mn})^{0.5} (\overline{T} + 17.8)}{\lambda} \tag{4}$$

where E_0 is the potential evapotranspiration (mm day^{-1}), H is the extraterrestrial radiation (MJ m^{-2} day^{-1}), T_{mx} the maximum air temperature (°C), T_{mn} the minimum air temperature (°C), $\overline{T}$ the mean air temperature and λ the latent heat of vaporization (MJ Kg^{-1}).

Actual evapotranspiration is then calculated as a function of potential evapotranspiration, water storage in the plant canopy, leaf area index, sublimation and evaporation from the soil, according to the equations specified in (Neitsch et al., 2005).

3.1.3 Surface runoff

Surface runoff occurs when soil is saturated by water (saturation excess) or the rate of water influx is higher than the infiltration rate (infiltration excess). For infiltration excess, surface runoff will therefore depend on how the model computes infiltration.

In RHESSys infiltration is computed using the equation proposed by (Philip, 1957):

$$q_{\mathrm{infil}} = It_{\mathrm{p}} + S_{\mathrm{p}}\sqrt{t_{\mathrm{p}} + t_{\mathrm{p}}} + K_{\mathrm{sat_s}}(t_{\mathrm{d}} - t_{\mathrm{p}}) \quad \text{for} \quad t_{\mathrm{d}} > t_{\mathrm{p}}$$
$$q_{\mathrm{infil}} = It_{\mathrm{d}} \quad \text{for} \quad t_{\mathrm{d}} < t_{\mathrm{p}} \tag{5}$$

where q_{infil} is infiltration; I and t_{d} are input intensity and duration; $K_{\mathrm{sat_s}}$ is saturated hydraulic conductivity at the wetting front. S_{p} is sorptivity and t_{p} is time to ponding. For saturation excess, runoff is generated when the water table of a given spatial unit has reached the surface. In this study region, this commonly occurs in riparian areas near the stream. RHESSys computation of vertical drainage and lateral moisture redistribution determines the saturation deficit for each spatial unit. RHESSys also computes shallow subsurface throughflow which can contribute to streamflow. Additional details are provided in Tague and Band (2004) and Tague et al. (2008).

In SWAT, the SCS curve number method is used for estimating surface runoff. The equation (SCS, 1972) is:

$$Q_{\mathrm{surf}} = \frac{\left(R_{\mathrm{day}} - I_{\mathrm{a}}\right)^2}{\left(R_{\mathrm{day}} - I_{\mathrm{a}} + S\right)} \tag{6}$$

where Q_{surf} is the accumulated runoff or rainfall excess, R_{day} is the rainfall depth for the day, I_{a} is the initial abstractions which includes surface storage, interception and infiltration prior to runoff, and S is the retention parameter, which depends on the SCS curve number of the day.

Runoff will occur when $R_{\mathrm{day}} > I_{\mathrm{a}}$, and the SCS curve number is a function of the soil's permeability, land use and antecedent soil water conditions. Typical curve number values for different conditions are given in the SWAT manual (Neitsch et al., 2005).

Title Page
Abstract Introduction
Conclusions References
Tables Figures
◀◀ ▶▶
◀ ▶
Back Close
Full Screen / Esc
Printer-friendly Version
Interactive Discussion

3.2 Input data

One of the advantages of comparing RHESSys and SWAT models is that the basic input data requirements are the same, i.e., a terrain elevation model, land cover types, soil classes, daily precipitation and daily maximum and minimum temperature.

Climatic data (daily precipitation, minimum and maximum temperature) were obtained from the Spanish Meteorological Agency (AEMET, Agencia Estatal de Meteorología) at 15 climatic stations located within and close to the watershed. Hydrological data used for calibration and validation purposes were provided by the Ebro Basin Authorities (*Confederación Hidrográfica del Ebro*).

The land cover types were obtained from the Spanish National Forest Inventory (1997–2007). A reclassification of the original land-cover types was necessary in order to reduce the number of classes. This was done on the basis of similarities in the hydrological response between classes, for example all deciduous forest species (e.g. *Fagus sylvatica, Corillus avellana, Betula pendula*) were merged into "deciduous forest" class, or the different kind of coniferous species (e.g.: *Pinus sylvestris, Pinus nigra, Pinus uncinata*) were merged into "pine forest". The final number of land-cover classes was 9, including six vegetation classes: deciduous forest, pine forest, oak forest, crops, shrubs, and pasture; and three non-vegetation classes: bare soil-rock, urban areas and water bodies (Fig. 1b).

The soil type layer was obtained from the European Soils Database (Joint Research Centre, http://eusoils.jrc.ec.europa.eu/). Soil classes are provided together with an alphanumeric database that contains information about the physical and chemical characteristic of the soils. From these we obtained the hydrological properties of soils (e.g.: available water content, saturated hydraulic conductivity) that are needed by the models to simulate the paths of water once it reaches the soil. The predominant soils in the watershed are leptosols, characterized by shallow profiles and gravelly textures, and in a lesser extent cambisols, with a finer texture and therefore more impermeability (Fig. 1c).

3.3 Model calibration

Calibration is a critical process to assess model performance as it involves the adjustment of model parameters until a reasonable statistical agreement between observed and simulated outputs is obtained. In this case we performed calibration based on observed stream flows in the outlet of the basin for the period 1996–2006. Each model was calibrated separately based on standard methods, and calibration included two phases In the first phase, for both models, parameters that control the development of the foliar mass in vegetation where manually adjusted until the models simulated reasonable values of leaf area index (LAI) according to literature review (Llorens and Domingo, 2007; White et al., 2000). LAI is a key variable controlling the amount of water from precipitation reaching the soil through the vegetation canopy, as well as the amount of evapotranspiration from the canopy. Having realistic values of LAI is essential when simulating effects of land-use changes on water balance components. For SWAT, LAI is estimated in the context of a plant growth model that considers the accumulation of heat units (temperature-based) that let the plant's foliar mass develop until a maximum LAI is reached; the plant becomes then dormant in the winter months, when the LAI is set the minimum value. Plants resume growth when daily air temperature exceeds a minimum temperature required and heat units restart accumulating. More details on heat units and leaf area index estimation for SWAT can be found in Neitsch et al. (2005) RHESSys, on the other hand, contains a dynamic carbon cycling model that is fully coupled to the hydrology model. The model estimates photosynthesis and plant and soil respiration at a daily time step and allocates carbon to leaf, root and stem growth. The model also estimates daily and seasonal turnover of these plant components. Land cover classes discussed above are used to select ecophysiological parameters from available RHESSys parameter files. Vegetation carbon stores, including leaf carbon, were initialized by running the model for 351 yr (spinup) prior to the simulation period. A longer meteorological forcing record is obtained by repeating available historic data for this vegetation spinup. A specific leaf area parameter that varies by vegetation type is used to compute LAI from leaf carbon. Details of the carbon cycling process model are available in Tague and Band (2004) and more detailed discussion of spinup and validation of the couple carbon-hydrology in Zierl et al. (2007) and Tague et al. (2009).

The second phase included the automatic (multiple iterations) calibration of parameters For RHESSys, a Montecarlo simulation (up to 1600 runs) was performed, including the random combinations of two pairs of parameters responsible for the hydrological properties of the soil, as recommended in RHESSys online manual (http://wiki.icess.ucsb.edu/rhessys/Main_Page) and Tague and Band (2004). SWAT was calibrated based on AMALGAM (Vrugt and Robinson, 2007), which is a combination of four different algorithms of parameters optimization adapted for SWAT by Rahman et al. (2013). A number of soil parameters as well as parameters responsible for snowfall and melting processes to occur were calibrated. For the two calibration processes the objective criteria selected for parameter optimization were the Nash–Sutcliffe Efficiency (NSE, Nash and Sutcliffe, 1970) and Percent Bias (PBIAS) statistics, which are amongst the statistical indices recommended by Moriasi et al. (2007) for model performance evaluation. NSE measures the variability of the model residuals with respect to the variability of the observations, and implicitly compares the performance of the hydrological model used, to that of a hypothetical model that yields as predictions the mean (constant) value of observations (Schaefli and Gupta, 2007). Its values range from $-\infty$ to $+1.0$, with 1.0 being optimal performance, 0.0 indicating equal performance of the model to that of the mean of observations and $\mathrm{NSE} < 0.0$ indicating totally unacceptable performance. PBIAS measures the deviation, in percentage, of simulated data with respect to observed data. $\mathrm{PBIAS} = 0.0$ indicates accurate simulation; positive values indicate model underestimation bias and negative values indicate model overestimation bias. Recommended values for *good* model performance are: $0.65 < \mathrm{NSE} \leq 0.75$ and PBIAS between 10 and 15 %. For *very good* model performance statistics are: $\mathrm{NSE} \geq 0.75$ and $\mathrm{PBIAS} < \pm 10\,\%$ (Moriasi et al., 2007). More information about objective criteria and the equations for the two used statistics can be found in the aforementioned works.

After calibration, performance of calibrated parameters needs to be assessed for an independent set of data (different time period) with no further adjustment of parameters. This is referred to as "validation", and for this work we selected the time period 1986–1995. In Fig. 2 we show the performance of the two models after parameter optimization, for the calibration and the validation periods. For both RHESSys and SWAT, simulated river flows show a high level of agreement with observations after the calibration of parameters, with $\mathrm{NSE} > 0.8$ for the calibration period and $\mathrm{NSE} \approx 0.7$ for the validation period, and PBIAS values $< 15\,\%$ A little discordance between models is observed, however, according to PBIAS. While RHESSys slightly overestimates river flows for the calibration period and underestimate for the validation period, SWAT underestimates, on average, river flows for both calibration and validation periods. Despite differences, both models are able to accurately simulate the water yield of the watershed, respecting the variability of river flows, and with small levels of bias.

3.4 Climate and land-use scenarios

The models were run and calibrated for observed climate, land-cover and soil types in the watersheds. For assessing the sensitivity of each model's outputs to land-cover and climate changes, the models were then re-run (keeping constant the calibrated parameters) for a number of land-use scenarios and the outputs from various climate models.

For climate change simulations we considered the outputs of three regional climate models (RCMs) for the time slice 2021–2050, from the ENSEMBLES project database (http://www.ensembles-eu.org/, Hewitt, 2004). This comprises a number of transient simulations of climate from 1950 to 2100 at high spatial resolution ($25\,\mathrm{km}^2$ grid size; approximately 0.2°) for the A1B scenario of moderate greenhouse gas emissions. From the 12 RCM's used in the ENSEMBLES project, we selected three different RCMs that captured the range of temperature increases projected for the aforementioned time-slice with respect to control period (1970–2007). We selected the following RCM's (driving Global Climate Model): C4I (HadCM3Q16), which projects the highest temperature increase (3.1 °C); DMI (ECHAM5-r3), which projects the lowest increase (1.1 °C); and SMHI (HadCM3Q3), which provides results located around the median (1.46 °C) of the temperature increase inter-model range. The three models show fairly good statistical agreement with observations for the control period for maximum and minimum temperatures. For precipitation only DMI is capable of reproducing the statistical characteristics of the observations, whereas C4I and SMHI present poorest performance (see the Taylor diagram in Fig. 3). Table 1a shows the projected changes in temperature and precipitation for each RCM.

The current land-use distribution in the watershed is the result of various anthropogenic and natural processes that have occurred during the last five decades, including the diminishing and abandonment of rural activities such as cropping and grazing, or the afforestation of slopes for economic and environmental purposes. This has led to an expansion of forested area, which nowadays occupies nearly 50 % of the watershed's area. The two other predominant land-uses are agricultural lands (14 %) in the valley bottom and sub-alpine pastures (13 %) in the high elevated areas of the watershed. Besides the current land-use scenario, two other potential scenarios were generated, based on realistic assumptions. On the one hand, we considered a further increase of altitudinal forest expansion. The current tree line is below its natural limit due to human intervention in the past to gain land for feeding livestock. However, currently land is undergoing afforestation as a consequence of reduced grazing and warmer temperatures (García-Ruiz et al., 2011). Therefore, the "re-vegetation scenario" includes the substitution of mountainous shrub and sub-alpine pasture by pine forests up to 2000 m, and the substitution of pastures by shrub (pine forest near the tree line limit, therefore with shrub-like morphology) up to 2200 m (the altitude limit for the *Pinus uncinata* in the Pyrenees stands around 2200–2400 m according to Rivas-Martínez, 1968). The third scenario considers the potential vegetation after a wildfire. Wildfires have been a historical agent for shaping landscapes and ecosystems in the

Mediterranean. Here we consider a post-fire scenario in a high altitude sector of the basin, in which forest has disappeared and shrub lands have colonized the soil, thus becoming the predominant feature of land-cover together with the mountainous pastures. The extension of each changing class for the different scenarios is shown in Table 1b.

The combination of the three land-use scenarios and the four climate scenarios (current and three RCMs), leads to 12 (1 baseline + 11 potential) scenarios, for which a number of water balance components were simulated, and compared between the two hydrological models The comparison of the different components was undertaken at two spatial scales: (1) the water yield (river discharges in hm^3) comparison was carried out for the entire watershed; (2) the surface runoff, snowpack water content, and evapotranspiration, were compared at a sub-basin scale, as this is the spatial unit at which the models generate those variables. We selected a sub-basin with relatively small size within the basin, to facilitate the performance of model runs and avoid the influence of stream flow aggregation processes which could mask the sensitivity of water balance components to changing input conditions. The selected sub-basin included a mosaic of land-uses (deciduous forest, pine forest, shrub lands, pasture...) and a high mean altitude. We focused on a high altitude sub-basin where snowfall and snowmelt occur to highlight the sensitivity of these processes to climate scenarios. The selected sub-basin is located in the north-west sector of the watershed (Fig. 1), has 44.6 km^2 of extension and a mean altitude of 1580 m a.s.l.

4 Results

4.1 Changes in water yield at the watershed scale

Figure 4 shows the monthly and annual changes in water yield at the basin scale between the simulation for current conditions and the simulations for the climate and land-use scenarios, for averages of 20 yr periods (observation period: 1986–2006). We first observe that the largest overall change is exhibited by the climate conditions simulated by the SMHI model, with a decrease in annual water yield of 15 % and 13 % for the SWAT and RHESSys models respectively. The reason for this is that, as shown in Table 1b SMHI projects the largest decrease (16 %) of precipitation in autumn, which together with winter is the moist season of the year in the study area. Besides the decrease in annual water yield, which is a common feature for all climate scenarios, the most manifest change is the loss of the spring peak flows, and the consequent increase of winter flows. This change is most remarkable for C4I, which is the model that projects the strongest warming at both seasonal and annual scales (Table 1b). Thus warmer temperatures will reduce the ratio of winter precipitation falling as snow and will trigger an earlier melting of snowpack as well, thus explaining the observed shift in the hydrograph. To better appreciate the shift in the timing of flows under warmer conditions we have calculated the day of center of mass (D_{cm}: the day of the water year in which the 50 % of the total streamflow occurs) for each scenario (Table 2). We thus observe that for SWAT, in the most optimistic warming scenario scenario (DMI), the 50 % of volume of water would be reached only 5 days earlier than under current conditions, whereas for the most pessimistic scenario (C4I), this would happen 33 days earlier, indicating a dramatic shift in the stream flows timing. For RHESSys the changes are less accentuated with D_{cm} occurring 6 and 22 days earlier for DMI and C4I scenarios, respectively. Although both SWAT and RHESSys show the same patterns of change in water yield with varying climate conditions, this first results show that SWAT always projects a larger decrease in annual river flows than RHESSys, when forcing climate variables to change.

For the re-vegetation scenario (increase of forest altitude limit up to 2200 m) estimates show annual water losses of 7.4 % for SWAT and 10 % for RHESSys, with the decrease being greater in autumn and spring months. On the contrary, when considering a scenario where forest is substituted by shrubs (post-fire vegetation) in the western part of the basin, an increase in river flows is observed, with increases being greater for RHESSys (10 %) than for SWAT (2.4 %) As discussed in detail in Sect. 4.2, these changes have to do with the impact of land-use on evapotranspiration, and in this case RHESSys produces larger changes than SWAT.

We thus see in a first approach that SWAT seems more sensitive to changes in climate than RHESSys, and RHESSys is more sensitive to land-use change than SWAT in terms of the changes projected in water yield. In order to quantify these differences we plot in Fig. 5 the seasonal (monthly-averaged) changes in stream flow for the 11 altered scenarios in comparison with the control scenario, for both SWAT (left-side semicircles) and RHESSys (right-side semicircles). An overall look at the plot confirms the previous observation (i.e. greater sensitivity of SWAT and RHESSys to climate change and land-use change, respectively). These model differences can also be seen when combined climate and land-use scenarios are considered, and any decrease/increase in water yield will depend on the scenario and hydrological model considered. For example, in winter, SWAT shows larger water yield increase when only climate variables are changed, but when considering a post-fire scenario the increase is larger for RHESSys for current and DMI climate scenarios. For the re-vegetation scenario, increased forest cover counters the effects of increasing temperatures for both models and a decrease of water yield is observed, except for the most extreme warming scenario (C4I). For the other seasons a decrease in water yield is evident for both RHESSys and SWAT and for all scenarios, except for the post-fire scenario. Thus for winter through summer, the models agree on the direction of change but differ only in terms of the magnitude of change. For the post-fire scenario, model estimates differ both in the direction of change and in the magnitude of that change. In the case of SWAT, only when climate conditions remain unchanged, does the post-fire scenario show an increase in water yield; for RHESSys post-fire increases occur only for spring stream flows.

In the previous analyses the effect of climatic forcing on stream flow was observed. Those simulations included, however, the changes in both temperature and precipitation simultaneously, which can obscure the hydrological effect of the climatic variables when considered in isolation. In the next analysis we run the hydrological models by changing the climatic variables within the same range given by the RCMs, but only one or the other, i.e. changing seasonal temperatures according to values in Table 1a and maintaining current precipitation values, and vice versa. For an easier visual interpretation results of changes in stream flow were interpolated (using splines) in the 2-dimensional space, in order to create the surface plots of Fig. 6 in addition to the greater amount of change in SWAT compared to RHESSys already mentioned, we also observe how the patterns of change differ among seasons and models, when considering changes in the climatic variables. In winter we observe how the precipitation change driven by RCMs is almost negligible, thus implying that the positive change in stream flow is driven essentially by the increase in temperatures. However the surface trend shows how river flows start to increase only when temperature is raised by more than 0.5–1.0 °C. Below these values, precipitation is responsible for the decrease in stream flows. In the case of winter we observe how SWAT and RHESSys exhibit the same patterns of change, albeit with differences in magnitude. In spring, the same can be said for the SWAT and RHESSys intercomparisons (i.e. same pattern, different magnitude) and we see how the pattern of change in stream flow is driven in an almost symmetrical fashion by increasing temperatures and decreasing precipitation. In summer, we find the same pattern of change as in spring, i.e., a decrease in stream flow resulting from less precipitation and warmer temperatures (and thus enhanced evapotranspiration). However in the case of RHESSys the influence of temperatures is smaller, as indicated for the more vertical contour lines of the plot. For autumn the pattern of change is opposite to that of spring. When decreasing precipitation, stream flows also decrease, whereas increasing temperatures have the opposite effect, i.e., increasing stream flows. The reason for this behavior is related to the effect of temperatures on snow accumulation. In late autumn (October–November) snowfalls are already present in the high parts of the watershed, thus an important part of incoming precipitation remains locked within the snowpack and does not become runoff until spring. When increasing temperatures the fraction of rainfall to snow precipitation will increase and thus the amount of accumulated snow will be reduced. Therefore this precipitation will directly be converted to runoff, triggering the observed increase in autumn stream flows. This behavior is more evident for RHESSys than for SWAT, although again SWAT simulates the largest reduction of stream flow.

In this sub-section the different sensitivity of stream flow to land-use and climate changes between SWAT and RHESSys has been highlighted, and in general we have demonstrated that SWAT produces larger changes in stream flow when climate variables are forced to change while RHESSys yields greater changes when land-cover structure is changed. Taking into account that originally RHESSys produces an overall overestimation of flows and SWAT and overall underestimation (see PBIAS statistics in calibration) compared to observations, a systematic divergence between the two models is present. However, on the basis of results from these analyses, an increase or reduction of this divergence can be expected when considering the effects of climate and land-use changes on stream flow. Thus, in Fig. 7 we observe that under climate change scenarios, the divergence between SWAT and RHESSys usually decreases (blue figures) during the first half of the hydrological year, and drastically increases (red figures) during the second half, especially in the peak flows of the spring and summer. However, as temperature increases are higher (from DMI to C4I scenarios) there is a predominance of enhanced ranges of divergence between SWAT and RHESSys. In the re-vegetation scenario, the differences in results between the two models are generally reduced when compared to the control simulations, and the opposite is observed for the post-fire scenario.

4.2 Changes in water balance components at the sub-basin scale

The most remarkable changes observed under climate and land-use scenarios are the shifting of spring peak flows when increasing temperatures, the loss of water yield given by reduced precipitation, or the increase/decrease of water yield when land-cover scenarios are taken into account. Results indicate that the quantity of snowfall/snowmelt as well as the evapotranspiration (which accounts for the water evaporated from soil and plants surface plus the water transpired by plants), are essential water balance components for understanding the processes underlying the observed stream flow changes.

For a better assessment of the behavior of water balance components under changing conditions a second set of analyses have been conducted at the sub-basin scale. In particular, this enables the effects of land-cover changes on stream flow to be analyzed in depth, as the proposed changes have a greater magnitude (in relative terms) in the selected sub-basin than in the whole watershed. In addition, the contribution of snowfall/snowmelt, surface runoff and evapotranspiration is better assessed at this smaller scale.

Figure 8a shows the daily (long-term average) snowpack water content (snow water equivalent, SWE, in mm) in the sub-basin and the change in the mean yearly values, between the control period and the three climate scenarios. We observe that for the control simulation, SWAT produces slightly greater values of SWE than RHESSys. However, when climate-change scenarios are considered, the amount of SWE decreases drastically, and as already seen for the stream flow analyses, the decrease is more pronounced for SWAT than for RHESSys. In this case, it is evident that the decrease in the amount of snow is closely related to the increase in temperatures induced by the climate models, as C4I (DMI) produces the greatest (smallest) loss of SWE. In Fig. 8b, the average amount of water loss by evapotranspiration (ET) from the subbasin simulated by SWAT and RHESSys is shown. Although the seasonal pattern is similar for the two models, we observe that SWAT produces higher values of ET throughout the year, this being the possible cause for lower stream flows simulated by SWAT than by RHESSys. When considering the two land-use scenarios, the changes in ET are much more pronounced for RHESSys than for SWAT, the first (latter) showing a yearly increase of 71 % (19 %) for the re-vegetation scenario and a decrease of 34 % (−6 %) for the post-fire scenario. These differences also seem to explain the greater sensitivity of stream flow to changes in land-cover in RHESSys compared to SWAT. The same can be applied when we look at the sensitivity of the surface runoff (overland flow) to changes in land-cover (Fig. 8c). Regarding this variable, the differences between models are even larger. The two models reproduce the same intra-annual variability; however, RHESSys yields larger amounts of runoff than SWAT. When changing land-use the two models respond in the same manner, i.e. decreasing runoff for the re-vegetation scenario, and increasing runoff for post-fire scenario, but again RHESSys produces the largest amount of change.

The effect of land-cover changes on stream flow are well captured by the models, although RHESSys shows more sensitivity than SWAT. A last experiment was carried out in order to investigate more thoroughly the response of water yield and evapotranspiration to changes in land-cover, and to assess differences between the two models. In the selected sub-basin, the land-use "pasture" was substituted by "pine forest" gradually i.e. 10 % of pasture extension into forest, 20 %, 30 % . . . and up 100 %. For each of these 10 land-use scenarios the water yield and the mean evapotranspiration of the basin were compared with current land-use scenario. Figure 9 shows the results in relative changes for the monthly (surface plots) and yearly (line plots). As expected, the changes generated by RHESSys are of greater magnitude than those of SWAT. However, the major insight from this analysis is the evidence of a different behavior of the hydrological variables between the two models, when the forest expansion is increased in a linear way. The monthly pattern of change shows that the greatest decrease (in relative terms) in stream flow occurs in summer months for SWAT and between late summer and winter for RHESSys. Moreover, whereas SWAT yields a decrease in stream flow for all months and all scenarios, in RHESSys a slight increase is observed in spring months when pasture is change into forest up to a 50 % level. When looking at the yearly changes (right plots) we observe that the response of stream flow to increased forest cover is perfectly linear for SWAT. RHESSys on the contrary, shows a more complicated pattern with the slope of the curve (intensity of flow decrease) become flatter when reaching a 50 % change in pasture-to-forest, with a steep decrease observed thereafter. For evapotranspiration the same feature is observed, although with the greatest difference amongst the models. A linear increase in ET is given by SWAT when forest cover is increased linearly, and a sharp change is observed for ET in RHESSys again from the 50 % change of pasture to forest. On a monthly basis, the two models yield a similar pattern of change in ET, but the amount of increase for RHESSys is one order of magnitude greater than for SWAT (see the values of color scale).

5 Discussion

Substantial research has been carried out in the field of hydrology in order to predict the future behavior of river flows under changing environmental conditions, especially in the climate variables and the land-cover distribution. The process-based hydrological models are the most widely used tool for hydrological forecasting in both scientific and management fields, as they allow simulating through physical relationships a number of processes and variables that integrate the water cycle. In general terms, a decrease of river flows can be expected according to the two models used in this work, if climate and land-use evolve as predicted. The process of re-vegetation in the studied area and other Mediterranean mountains is likely to continue in the manner discussed in this paper, i.e. shrubs evolving to forest and sub-alpine pastures being colonized by shrubs (García-Ruiz and Lana-Renault, 2011; García-Ruiz et al., 2011). Moreover, climate projections agree in emphasizing the fact that the Mediterranean will become a hotspot of climate warming in future decades (Solomon et al., 2007; Giorgi, 2006) and mountains are expected to suffer both an increase in temperatures and a decrease in precipitation (Bravo et al., 2008). According to the SWAT model, climate change will have greater impacts on the availability of water resources than land-cover changes. This fact has been emphasized by Koeplin et al. (2013) in a study on the Swiss Alps, although the latter will be affected by increasing glacier melting, which is not the case of the Pyrenees. Similar conclusions have been reported in other areas of the world when simulating stream flows under climate and land-cover scenarios with SWAT (Wang et al., 2008; Li et al., 2009) or other models (Legesse et al., 2003). However according to RHESSys land-use changes can have equal or even larger impacts on water resources than changes in the climate variables, in this specific environment. This highlights the importance of considering the combination of scenarios in order to understand the range of impacts of environmental changes in the future availability of water resources (Tong et al., 2012; Koeplin et al., 2013).

Despite the good performance of hydrological models to simulate stream flows in a range of environments, a number of uncertainties nevertheless remain. One of the aims of this work has been to highlight the fact that another source of uncertainty in hydrological forecast resides in the choice of the hydrological model to be used. The two compared models have been previously applied in mountainous environments, and seem adequate to simulate water yield and other hydrological variables under changing conditions at different spatial scales. RHESSys has been successfully applied to simulate transpiration (Christensen et al., 2008), to assess the impacts of climate change on water yield (Zierl and Bugmann, 2005) or to simulate snow distribution in different mountain regions of the world (Hartman et al., 1999), amongst other applications. SWAT, which was primarily developed for improving agricultural and irrigation management, has been successively updated and is able to reproduce the water cycle in mountainous and snow-dominated environments (Fontaine et al., 2002; Rahman et al., 2013; Pradhanang et al., 2011; Debele et al., 2010; Zhang et al., 2008). We demonstrate that even when the two models have been calibrated, and therefore can satisfactorily reproduce the stream flows of a given river basin, their forecast for future availability of water under hypothetical climate and land-use conditions may differ substantially from each other. Although the direction of changes estimated by the models was usually consistent, the magnitudes of these changes were substantially different. In the case of this study, SWAT tends to produce larger changes in hydrological variables under induced changes in climate variables, and RHESSys tends to produce larger hydrological changes under induced land-use changes. As mentioned in the methods section (3.1), the main equations for hydrological processes and water partitioning of the two compared models (snowmelt, canopy interception, evapotranspiration and surface runoff generation) are different. These differences could be the cause for the differing sensitivity to climate and especially to land-use change. To provide examples we analyzed, at the sub-basin scale, the behavior of different variables (snow water equivalent, evapotranspiration and surface runoff) that are essential components of the water balance. Regarding ET, we observe that it is the key element for understanding the effect of land-use changes on water yield. Forest expansion enhances evapotranspiration given the larger surface of plant canopy to retain water from precipitation (interception) as well as for the increased amount of water used by plants for their biological activity (Crockford and Richardson, 2000; Zhang et al., 2001). This consequently implies less water available for runoff and an overall decrease in the catchment water yield. Our results indicate that ET and water yield show a linear response when forest is gradually increased in the SWAT model, and a non-linear response is observed for RHESSys, where an abrupt change is observed once a certain threshold of forest increase is reached. These differences in ET estimates are most likely related to the way that both models compute actual evapotranspiration. SWAT estimates actual evapotranspiration through empirical equations and as a function of potential evapotranspiration, water held in plant canopy or sublimation amongst other variables. On the contrary RHESSys has a more process-based evapotranspiration estimate, with a more complex representation of canopy controls on transpiration, through stomatal conductance, a time-varying rooting depth and sunlit and shaded leaves. While this representation may be more physiologically realistic it also requires additional parameterization that can introduce further error. Testing of model estimates against measured evapotranspiration data across a range of vegetation types would be required to determine whether or not the additional physiological realism in RHESSys actually produces more accurate estimates, relative to SWAT. Regarding snow, both models simulate a decrease of SWE when climate scenarios are considered, and this seems to be the main cause for the shifting peak flows. Under warmer conditions it is expected that the amount of precipitation falling as snow decreases, and that melting occurs earlier. Both signals are captured in the behavior of SWE for climate change scenarios, and these signals are subsequently transferred to the corresponding hydrograph. The shift in the peak flows is already a fact in many snow-dominated areas of the Mediterranean (García-Ruiz et al., 2011), and further changes in the future may require substantial modifications in the management of the numerous reservoirs in the region (López-Moreno et al., 2008), as the one located downstream of the studied area. Our estimates show greater reduction in snow with climate scenarios found using SWAT. Again, the RHESSys model is more physically realistic – accounting for both radiation and temperature driven melt –, but again further analysis would be needed to determine whether the additional parameterization associated with this complexity actually produces more accurate results.

It must be taken into account as well the original conception of the models, as RHESSys was conceived for simulating carbon, water and nutrients cycling in natural environments, whereas SWAT was in principle oriented to model water, sediment, or contaminant yields in crops and managed watersheds (Tague and Band, 2004; Neitsch et al., 2005). The question that arises from this observation is to what extent these divergences can be considered an overestimation or an underestimation from one model to another. In other words, is SWAT overestimating hydrological changes under climate conditions, or is RHESSys underestimating them? (The same argument is applicable to land-use changes). The answer to this question is difficult to provide based on the observations of this study, thus it certainly requires further research, and even comparisons with additional hydrological models in other areas and environments In the meanwhile it is the responsibility of model users to assess the uncertainty associated to model predictions and recognize the strengths and limitations of the model used.

Finally, our observations highlight that the degree of divergence (which can be considered as a degree of uncertainty) in the forecasted stream flow between the two models may be enhanced or reduced depending on the combination of climate change and land-use change scenarios This can also be related to the calibration process. In this particular case, the best calibrated parameters for RHESSys yielded a systematic overestimation of river flows, whereas for the optimal parameterization of SWAT, stream flows are systematically underestimated (when compared to observations). When revegetation is considered, stream flows are reduced in the two models, but to a greater extent in RHESSys, therefore the uncertainty range (i.e., the divergence between the two models) is in this case reduced. The opposite is observed when vegetation is removed. For the case of climate change scenarios the pattern is less clear but there is a trend towards increasing uncertainty when the projections for temperature increase are more severe (i.e., the C4I scenario). This circumstance could be different for example if other sets of parameterization had been used, in which the bias of modeled stream flow with respect to observations were of different magnitude or sign. This leads to the concept of "equifinality" (Beven, 2006) which in hydrological modeling refers to the possibility that different solutions or sets of model parameterizations may lead to optimal model performance, and it is considered as an important component of a model's uncertainty. It was not our intention in this work to evaluate the performance of different calibration solutions, but this will be done in further research in order to better understand the uncertainties related to hydrological modeling.

6 Conclusions

The components of water balance, including stream flow, evapotranspiration and snowpack water content were simulated for a Pyrenean watershed to assess its sensitivity to changes in climate and land-use change. Under climate change conditions (increasing temperatures and decreasing precipitation), stream flows will suffer reductions and shifting peak flows, leading to a dramatic change in the shape and magnitude of the hydrographs, which depends on the degree of severity of the climate scenario considered. When two hypothetical (but plausible) land-use scenarios are considered, stream flows (and evapotranspiration) are affected as well, i.e. a decrease of river flows and an increase in evapotranspiration are observed in the case of a re-vegetation scenario, and the opposite effect is observed when a post-fire vegetation scenario is considered.

The principal highlight of this work is the demonstration that model choice in general does not impact the direction of predicted change. However the magnitude and even the intra-seasonal patterns of these forecasted changes may differ substantially depending on the hydrological model used. In the case of this study, the broadly-used SWAT model shows larger sensitivity of water balance components to changes in climate variables, whereas the RHESSys model displays greater sensitivity to changes in land-cover. The response of flows to changes in precipitation and temperature shows a linear pattern in both models; however, when changes in land-cover are considered, SWAT exhibits a linear response and RHESSys a non-linear response. The combination of climate and land-use scenarios therefore yields a range of possibilities that are amplified when the two models are considered.

Projections of future availability of water resources contain a large number of uncertainties, and this work demonstrates that the choice of the hydrological model represents an additional source. Whereas it seems probable that water resources in the Mediterranean region will decrease in future decades as a consequence of climate and land-use changes, it is of great difficulty to ascertain an accurate magnitude of change. We identified evapotranspiration and snow accumulation and melt estimation as two areas where differences between models were particularly important. Further analysis of model estimates against observed data is needed to determine which model (if either) provides the more accurate estimates. Until this type of detailed model evaluation is done for this region, caution is recommended when interpreting results from hydrological modeling and implementing water policies based solely on model results.

Acknowledgements. This work has been made possible thanks to the financial support from the Spanish Government (Ministry of Education) through the postdoctoral program “Ayudas de movilidad postdoctoral en centros extranjeros (Orden EDU/2728/2011, de 29 de septiembre)” and the project CGL2011-27536/HID: “Hidrologia nival en el Pirineo central español: variabilidad espacial, importancia hidrológica y su respuesta a la variabilidad y cambio climático”, financed by the Spanish Commission of Science and Technology, and FEDER.

References

Abbaspour, K., Johnson, C., and Van Genuchten, M. T.: Estimating uncertain flow and transport parameters using a sequential uncertainty fitting procedure, Vadose Zone J., 3, 1340–1352, 2004.

Arnold, J. G., Srinivasan, R., Muttiah, R. S., and Williams, J. R.: Large area hydrologic modeling and assessment part I: model development 1, J. Am. Water Resour. As., 34, 73–89, 1998.

Beniston, M.: Mountain climates and climatic change: an overview of processes focusing on the European Alps, Pure Appl. Geophys., 162, 1587–1606, doi:10.1007/s00024-005-2684-9, 2005.

Beven, K.: A manifesto for the equifinality thesis, J. Hydrol., 320, 18–36, doi:10.1016/j.jhydrol.2005.07.007, 2006.

Beven, K. and Binley, A.: The future of distributed models: model calibration and uncertainty prediction, Hydrol. Process., 6, 279–298, doi:10.1002/hyp.3360060305, 1992.

Borah, D. K. and Bera, M.: Watershed-scale hydrologic and nonpoint-source pollution models: review of applications, T. ASAE, 47, 789–803, 2004.

Bravo, D. N., Araújo, M. B., Lasanta, T., and Moreno, J. I. L.: Climate change in mediterranean mountains during the 21st century, AMBIO, 37, 280–285, doi:10.1579/0044-7447(2008)37[280:ccimmd]2.0.co;2, 2008.

Butts, M. B., Payne, J. T., Kristensen, M., and Madsen, H.: An evaluation of the impact of model structure on hydrological modelling uncertainty for streamflow simulation, J. Hydrol., 298, 242–266, doi:10.1016/j.jhydrol.2004.03.042, 2004.

Chen, J., Liu, J., Cihlar, J., and Goulden, M.: Daily canopy photosynthesis model through temporal and spatial scaling for remote sensing applications, Ecol. Model., 124, 99–119, 1999.

Christensen, L., Tague, C. L., and Baron, J. S.: Spatial patterns of simulated transpiration response to climate variability in a snow dominated mountain ecosystem, Hydrol. Process., 22, 3576–3588, doi:10.1002/hyp.6961, 2008.

Crockford, R. and Richardson, D.: Partitioning of rainfall into throughfall, stemflow and interception: effect of forest type, ground cover and climate, Hydrol. Process., 14, 2903–2920, 2000.

Debele, B., Srinivasan, R., and Gosain, A.: Comparison of process-based and temperature-index snowmelt modeling in SWAT, Water Resour. Manag., 24, 1065–1088, 2010.

Fontaine, T., Cruickshank, T., Arnold, J., and Hotchkiss, R.: Development of a snowfall–snowmelt routine for mountainous terrain for the soil water assessment tool (SWAT), J. Hydrol., 262, 209–223, 2002.

García-Ruiz, J. M. and Lana-Renault, N.: Hydrological and erosive consequences of farmland abandonment in Europe, with special reference to the Mediterranean region – a review, Agr. Ecosyst. Environ., 140, 317–338, 2011.

García-Ruiz, J. M., López-Moreno, J. I., Serrano-Vicente, S. M., Beguería, S., and Lasanta, T.: Mediterranean water resources in a global change scenario, Earth-Sci. Rev., 105, 121–129, 2011.

Gassman, P. W., Reyes, M. R., Green, C. H., and Arnold, J. G.: The soil and water assessment tool: historical development, applications, and future research directions, T. ASABE, 50, 1211–1250, 2007.

Giorgi, F.: Climate change hot-spots, Geophys. Res. Lett., 33, L08707, doi:10.1029/2006gl025734, 2006.

Hargreaves, G. H. and Samani, Z. A.: Reference crop evapotranspiration from ambient air temperature, American Society of Agricultural Engineers, 1985.

Hartman, M. D., Baron, J. S., Lammers, R. B., Cline, D. W., Band, L. E., Liston, G. E., and Tague, C.: Simulations of snow distribution and hydrology in a mountain basin, Water Resour. Res., 35, 1587–1603, doi:10.1029/1998wr900096, 1999.

Hewitt, C. D.: Ensembles-based predictions of climate changes and their impacts, Eos. T. Am. Geophys. Un., 85, 566–566, 2004.

Jarvis, P.: The interpretation of the variations in leaf water potential and stomatal conductance found in canopies in the field, Philos. T. Roy. Soc. B, 273, 593–610, 1976.

Köplin, N., Schädler, B., Viviroli, D., and Weingartner, R.: The importance of glacier and forest change in hydrological climate-impact studies, Hydrol. Earth Syst. Sci., 17, 619–635, doi:10.5194/hess-17-619-2013, 2013.

Krysanova, V. and Arnold, J. G.: Advances in ecohydrological modelling with SWAT – a review, Hydrolog. Sci. J., 53, 939–947, 2008.

Lasanta-Martínez, T., Vicente-Serrano, S. M., and Cuadrat-Prats, J. M.: Mountain mediterranean landscape evolution caused by the abandonment of traditional primary activities: a study of the Spanish Central Pyrenees, Appl. Geogr., 25, 47–65, doi:10.1016/j.apgeog.2004.11.001, 2005.

Legesse, D., Vallet-Coulomb, C., and Gasse, F.: Hydrological response of a catchment to climate and land use changes in Tropical Africa: case study South Central Ethiopia, J. Hydrol., 275, 67–85, doi:10.1016/S0022-1694(03)00019-2, 2003.

Li, Z., Liu, W.-Z., Zhang, X.-C., and Zheng, F.-L.: Impacts of land use change and climate variability on hydrology in an agricultural catchment on the Loess Plateau of China, J. Hydrol., 377, 35–42, doi:10.1016/j.jhydrol.2009.08.007, 2009.

Llorens, P. and Domingo, F.: Rainfall partitioning by vegetation under Mediterranean conditions. A review of studies in Europe, J. Hydrol., 335, 37–54, doi:10.1016/j.jhydrol.2006.10.032, 2007.

López-Moreno, J. I. and García-Ruiz, J. M.: Influence of snow accumulation and snowmelt on streamflow in the Central Spanish Pyrenees, Hydrolog. Sci. J., 49, 787–802, 2004.

López-Moreno, J. I., Beniston, M., and García-Ruiz, J. M.: Environmental change and water management in the Pyrenees: facts and future perspectives for mediterranean mountains, Global Planet. Change, 61, 300–312, 2008.

Mayor, A. G., Bautista, S., Llovet, J., and Bellot, J.: Post-fire hydrological and erosional responses of a mediterranean landscpe: seven years of catchment-scale dynamics, Catena, 71, 68–75, doi:10.1016/j.catena.2006.10.006, 2007.

Monteith, J.: Evaporation and environment, Symp. Soc. Exp. Biol., 19, 205–223, 1965.

Moriasi, D., Arnold, J., Van Liew, M., Bingner, R., Harmel, R., and Veith, T.: Model evaluation guidelines for systematic quantification of accuracy in watershed simulations, T. ASABE, 50, 885–900, 2007.

Nash, J. and Sutcliffe, J.: River flow forecasting through conceptual models part I – a discussion of principles, J. Hydrol., 10, 282–290, 1970.

Neitsch, S., Arnold, J., Kiniry, J., Williams, J., and King, K.: Soil and water assessment tool: theoretical documentation, version 2005, Texas, USA, 2005.

Pappenberger, F. and Beven K. J.: Ignorance is bliss: Or seven reasons not to use uncertainty analysis, Water Resour. Res., 42, W05302, doi:10.1029/2005WR004820, 2006.

Pausas, J.: Changes in fire and climate in the Eastern Iberian Peninsula (Mediterranean Basin), Climatic Change, 63, 337–350, doi:10.1023/B:CLIM.0000018508.94901.9c, 2004.

Philip, J. R.: The theory of infiltration: 4. sorptivity and algebraic infiltration equations, Soil Sci., 84, 257–264, 1957.

Poyatos, R., Latron, J., and Llorens, P.: Land use and land cover change after agricultural abandonment – the case of a Mediterranean Mountain Area (Catalan Pre-Pyrenees), Mt. Res. Dev., 23, 362–368, 2003.

Pradhanang, S. M., Anandhi, A., Mukundan, R., Zion, M. S., Pierson, D. C., Schneiderman, E. M., Matonse, A., and Frei, A.: Application of SWAT model to assess snowpack development and streamflow in the Cannonsville watershed, New York, USA, Hydrol. Process., 25, 3268–3277, 2011.

Rahman, K., Maringanti, C., Beniston, M., Widmer, F., Abbaspour, K., and Lehmann, A.: Streamflow modeling in a highly managed mountainous glacier watershed using SWAT: the upper Rhone River watershed case in Switzerland, Water Resour. Manag., 27, 323–339, 2013.

Rivas-Martínez, S.: Estudio fitosociológico de los bosques y matorrales pirenaicos del piso subalpino, Publ. Inst. Biol. Apl., 44, 5–44, 1968.

Schaefli, B. and Gupta, H. V.: Do Nash values have value?, Hydrol. Process., 21, 2075–2080, doi:10.1002/hyp.6825, 2007.

SCS: Section 4: hydrology, in: National Engineering Handbook, Soil Conservation Service, 1972.

Shakesby, R. A.: Post-wildfire soil erosion in the Mediterranean: review and future research directions, Earth-Sci. Rev., 105, 71–100, doi:10.1016/j.earscirev.2011.01.001, 2011.

Solomon, S., Qin, D., Manning, M., Chen, Z., and Marquis, M.: Climate Change 2007: the Physical Science Basis: Contribution of Working Group I to the Fourth Assessment Report of the Intergovernmental Panel on Climate Change, Cambridge Univ. Press, New York, 2007.

Tague, C. and Band, L.: RHESSys: regional hydro-ecologic simulation system – an object-oriented approach to spatially distributed modeling of carbon, water, and nutrient cycling, Earth Interact., 8, 1–42, 2004.

Tague, C. and Peng, H.: The sensitivity of forest water use to the timing of precipitation and snowmelt recharge in the California Sierra: Implications for a warming climate, J. Geophys. Res.-Biogeo., 118, 875–887, doi:10.1002/jgrg.20073, 2013.

Tague, C., Grant, G., Farrell, M., Choate, J., and Jefferson, A.: Deep groundwater mediates streamflow response to climate warming in the Oregon Cascades, Climatic Change, 86, 189–210, 2008.

Tague, C., Seaby, L., and Hope, A.: Modeling the eco-hydrologic response of a Mediterranean type ecosystem to the combined impacts of projected climate change and altered fire frequencies, Climatic Change, 93, 137–155, 2009.

Tong, S. T. Y., Sun, Y., Ranatunga, T., He, J., and Yang, Y. J.: Predicting plausible impacts of sets of climate and land use change scenarios on water resources, Appl. Geogr., 32, 477–489, doi:10.1016/j.apgeog.2011.06.014, 2012.

Van Griensven, A. and Meixner, T.: Methods to quantify and identify the sources of uncertainty for river basin water quality models, Water Sci. Technol., 53, 51–59, 2006.

Vicente-Serrano, S. M., Lasanta, T., and Romo, A.: Analysis of spatial and temporal evolution of vegetation cover in the spanish central pyrenees: role of human management, Env. Manag., 34, 802–818, doi:10.1007/s00267-003-0022-5, 2004.

Viviroli, D. and Weingartner, R.: The hydrological significance of mountains: from regional to global scale, Hydrol. Earth Syst. Sci., 8, 1017–1030, doi:10.5194/hess-8-1017-2004, 2004.

Vrugt, J. A. and Robinson, B. A.: Improved evolutionary optimization from genetically adaptive multimethod search, P. Natl. Acad. Sci. USA, 104, 708–711, doi:10.1073/pnas.0610471104, 2007.

Wagener, T. and Gupta, H.: Model identification for hydrological forecasting under uncertainty, Stoch. Env. Res. Risk. A., 19, 378–387, doi:10.1007/s00477-005-0006-5, 2005.

Wang, S., Kang, S., Zhang, L., and Li, F.: Modelling hydrological response to different land-use and climate change scenarios in the Zamu River basin of northwest China, Hydrol. Process., 22, 2502–2510, doi:10.1002/hyp.6846, 2008.

White, M. A., Thornton, P. E., Running, S. W., and Nemani, R. R.: Parameterization and sensitivity analysis of the BIOME–BGC terrestrial ecosystem model: net primary production controls, Earth Interact., 4, 1–85, doi:10.1175/1087-3562(2000)004<0003:pasaot>2.0.co;2, 2000.

Zhang, L., Dawes, W. R., and Walker, G. R.: Response of mean annual evapotranspiration to vegetation changes at catchment scale, Water Resour. Res., 37, 701–708, 2001.

Zhang, X., Srinivasan, R., Debele, B., and Hao, F.: Runoff simulation of the headwaters of the Yellow River using the SWAT model with three snowmelt algorithms[1], J. Am. Water Resour. As., 44, 48–61, 2008.

Zierl, B. and Bugmann, H.: Global change impacts on Hydrological Processes in Alpine catchments, Water Resour. Res., 41, W02028, doi:10.1029/2004wr003447, 2005.

Zierl, B., Bugmann, H., and Tague, C. L.: Water and carbon fluxes of European ecosystems: an evaluation of the ecohydrological model RHESSys, Hydrol. Process., 21, 3328–3339, 2007.

Table 1. Climate and land-use scenarios considered in the study. (a) Changes in temperature (T) and precipitation (P) projected for the RCM's. (b) Absolute and relative extension of the land-uses classes in the current and hypothetical land-use scenarios. Only shown classes subject to change.

(a)	C4I		SMHI		DMI	
	ΔT (°C)	ΔP (%)	ΔT (°C)	ΔP (%)	ΔT (°C)	ΔP (%)
Winter	2.43	−0.47	1.94	−1.38	0.67	0.14
Spring	3.36	−7.82	1.87	−16.21	1.12	−0.38
Summer	3.12	−12.18	0.82	−0.10	1.61	−5.94
Autumn	3.46	−7.33	1.87	−16.21	0.87	−11.91
Annual	3.09	−28.31	1.46	−6.59	1.07	−4.82

(b)	Current		Re-vegetation		Post-fire	
	km^2	%	km^2	%	km^2	%
Deciduous forest	58.0	4.0	58.0	4.	34.1	2.4
Pine fores	525.9	36.5	881.8	61.3	403.6	28.0
Quercus forest	148.3	10.3	148.1	10.3	117.4	8.1
Pastur	191.6	13.3	11.7	0.8	191.6	13.3
Shrubs	205.5	14.3	28.1	2.0	387.0	26.8

Table 2. Change in the day (day of center of mass, D_{cm}) of the hydrological year in which 50 % of stream flow occurs (S_{50}). D_{cm} = 1: 1 October; D_{cm} = 365: 30 September.

climate/land-use	current			re-vegetation			post-fire		
	S_{50} (hm^3)	D_{cm}	change (days)	S_{50} (hm^3)	D_{cm}	change (days)	S_{50} (hm^3)	D_{cm}	change (days)
				SWAT					
current	331.0	156	–	305.7	155	−1	338.5	157	1
DMI	294.5	151	−5	271.1	149	−7	302.0	151	−5
SMHI	281.2	144	−12	259.3	142	−14	288.3	144	−12
C4I	283.6	123	−33	263.1	123	−33	291.6	124	−32
				RHESSys					
current	451.7	170	–	404.5	170	0	498.8	172	2
DMI	411.7	164	−6	365.9	164	−6	458.6	165	−5
SMHI	399.4	164	−6	356.4	164	−6	445.0	165	−5
C4I	406.7	148	−22	364.3	145	−25	451.6	150	−20

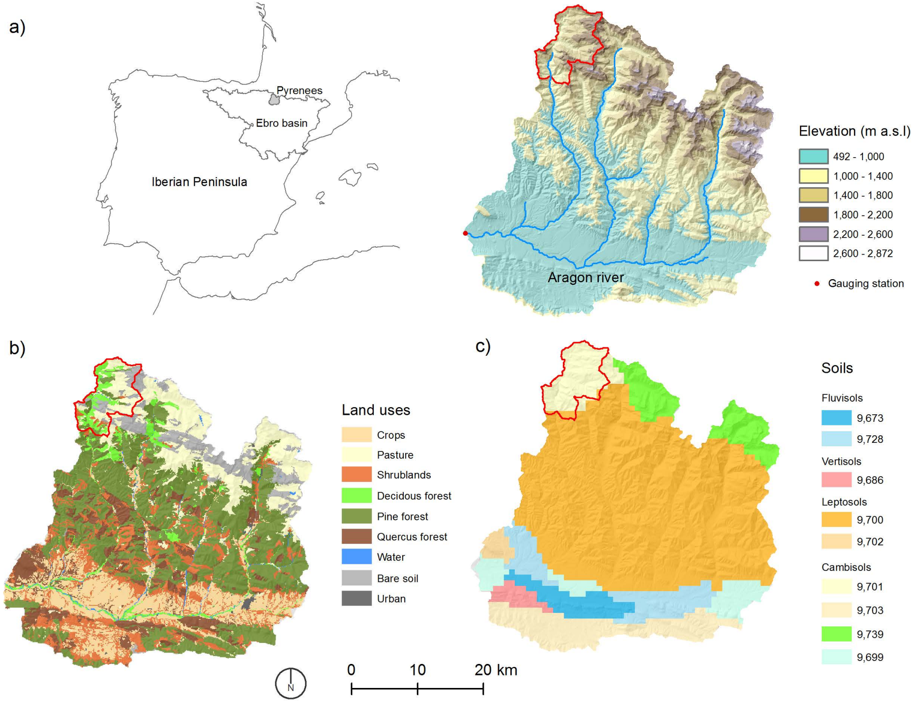

Fig. 1. Location and topography of the Aragon river watershed **(a)**, distribution of land-use categories **(b)**, and predominant soils **(c)**. Sub-basin for analysis of water balance components is shown in red.

Title Page
Abstract | Introduction
Conclusions | References
Tables | Figures
|◀ | ▶|
◀ | ▶
Back | Close
Full Screen / Esc
Printer-friendly Version
Interactive Discussion

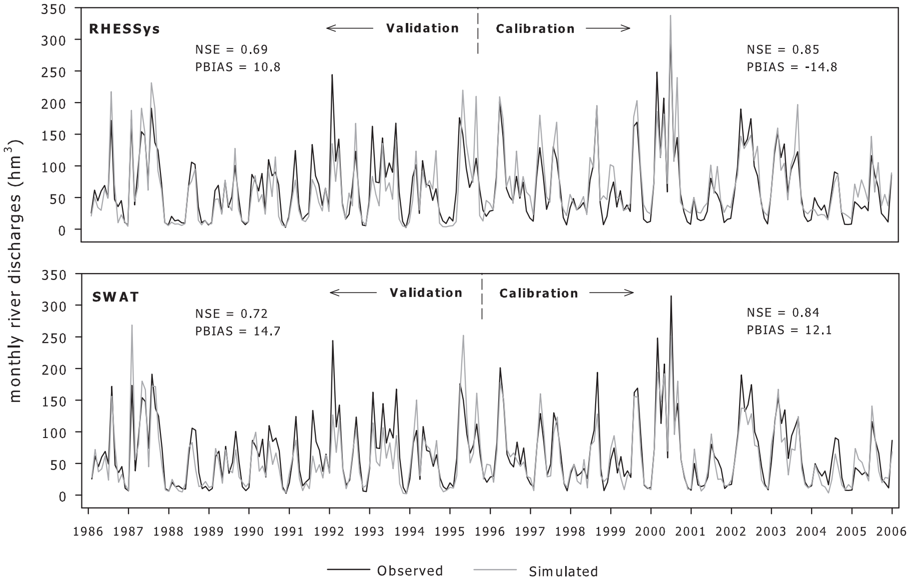

Fig. 2. Simulated vs. observed flows after parameter calibration. Agreement between observed and simulated river flows is assessed by NSE and PBIAS statistics.

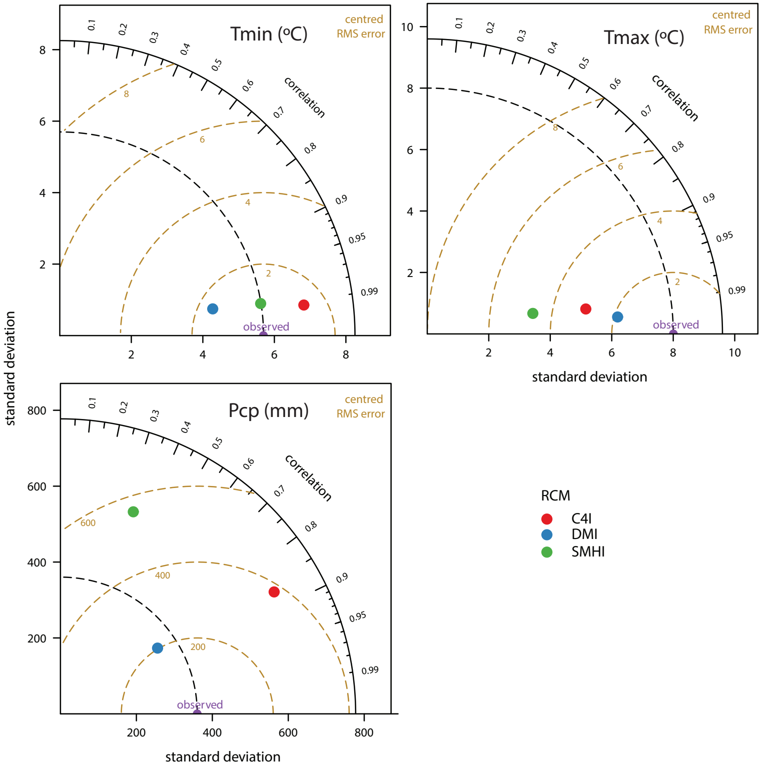

Fig. 3. Taylor Diagram showing the statistical agreement of the three RCMs with the observations, for minimum temperatures ($T_{\min}$), maximum temperatures ($T_{\max}$) and precipitation (Pcp). The statistical criteria for comparison include standard deviation, Pearson's correlation, and root mean squared (RMS) error. Diagram elaborated with R package "openair".

Title Page
Abstract
Introduction
Conclusions
References
Tables
Figures
◀▏
▶▏
◀
▶
Back
Close
Full Screen / Esc
Printer-friendly Version
Interactive Discussion

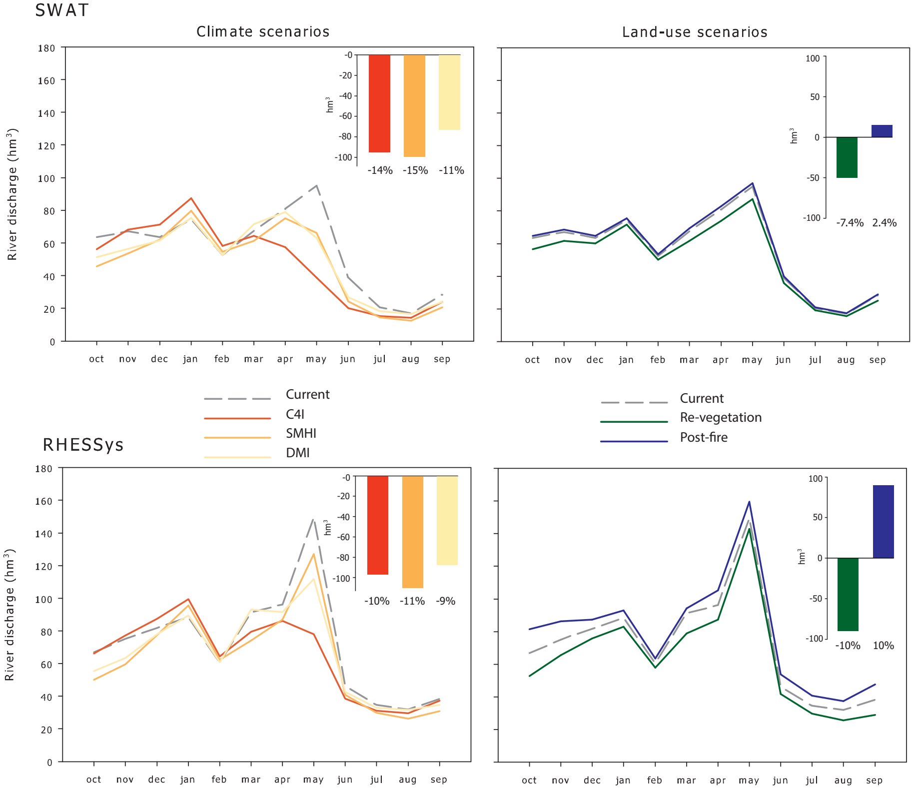

Fig. 4. Changes in river discharges between current conditions and climate (left panels)/land-use (right panels) scenarios, for the 20 yr simulations. Bar plots show the annual change in absolute (bar size) and relative terms (percentage value).

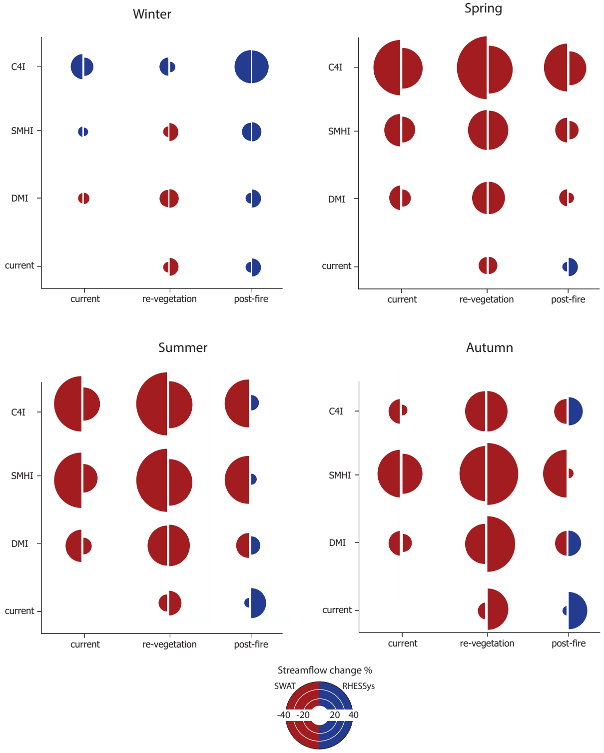

Fig. 5. Relative changes in stream flow between the simulation of current conditions and the simulations under climate and land-use change scenarios given by SWAT (left-hand-side semi-circles) and RHESSys (right-hand-side semicircles) models. Circle size indicates the amount of change; red and blue fills indicate negative and positive change, respectively.

HESSD

10, 11983–12026, 2013

Title Page
Abstract | Introduction
Conclusions | References
Tables | Figures
◀| |▶
◀ ▶
Back | Close
Full Screen / Esc
Printer-friendly Version
Interactive Discussion

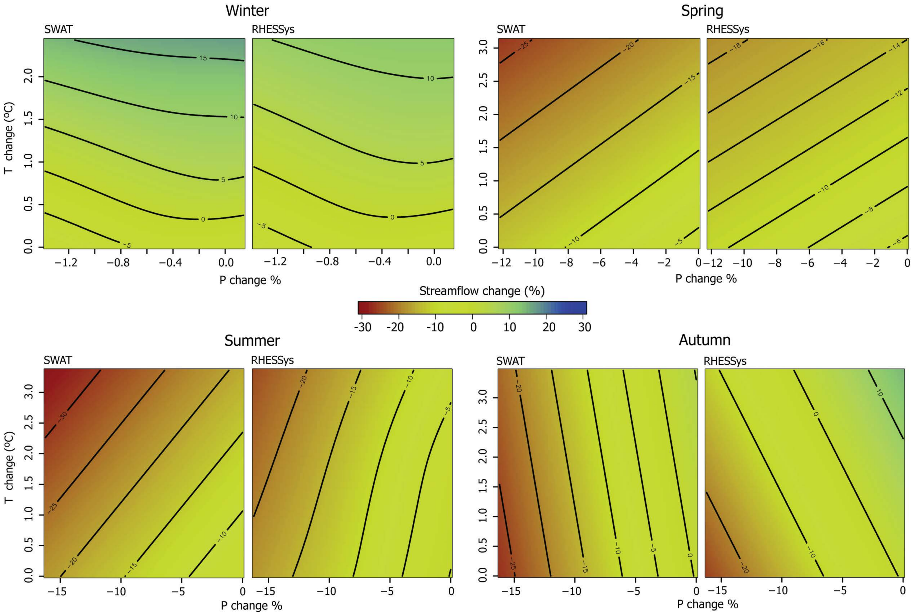

Fig. 6. Changes in seasonal stream flow driven by changes in temperature (*y* axis) and precipitation (*x* axis). Smoothed surface and contours were obtained by interpolating results with splines interpolation method.

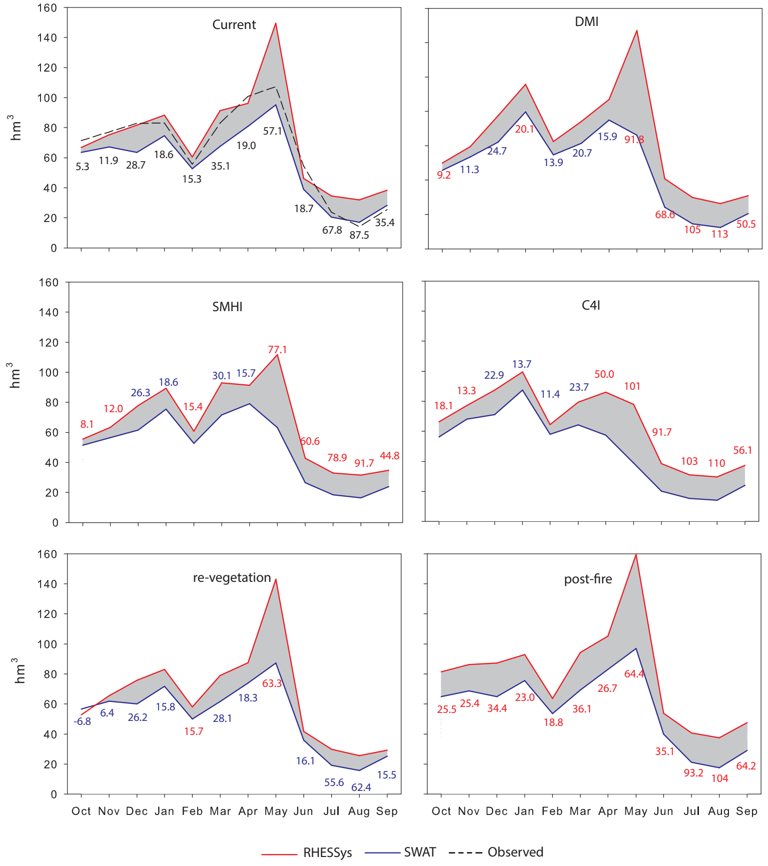

Fig. 7. Differences of stream flow simulations between the SWAT and RHESSys models. The grey band represent the absolute difference in hm^3, and the figures the relative difference in percent. The colors in the figures identify whether the difference is enhanced (red) or reduced (blue) in the climate and land-use scenarios with respect to the baseline scenario.

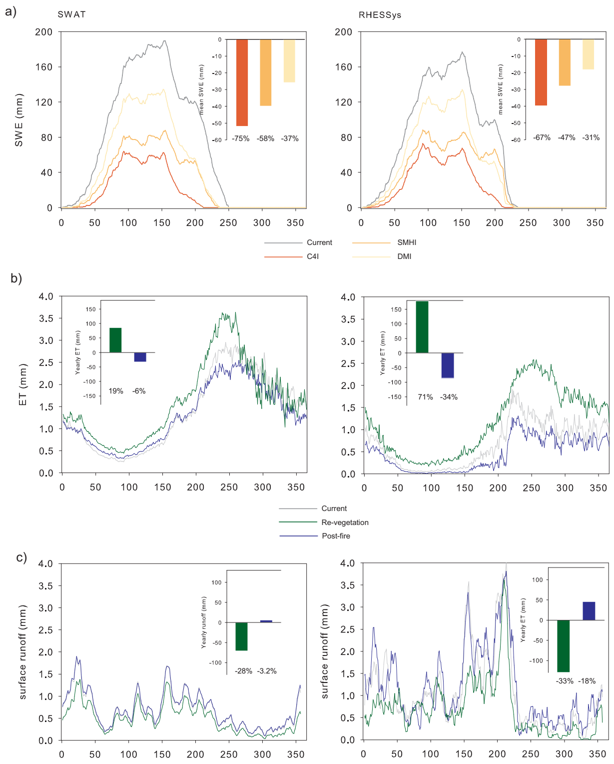

Fig. 8. Sensitivity of water balance components to climate and land-use changes. **(a)** Amount of water in the snowpack (snow water equivalent, SWE). **(b)** Water loss by evapotranspiration (ET). **(c)** Surface runoff (overland flow). Line plots show the average daily values (from 1 October to 30 September) for the 20 yr simulation period. Bar plots show the annual change in absolute (bar size) and relative terms (percentage value).

Title Page
Abstract | Introduction
Conclusions | References
Tables | Figures
◀◀ | ▶▶
◀ | ▶
Back | Close
Full Screen / Esc
Printer-friendly Version
Interactive Discussion

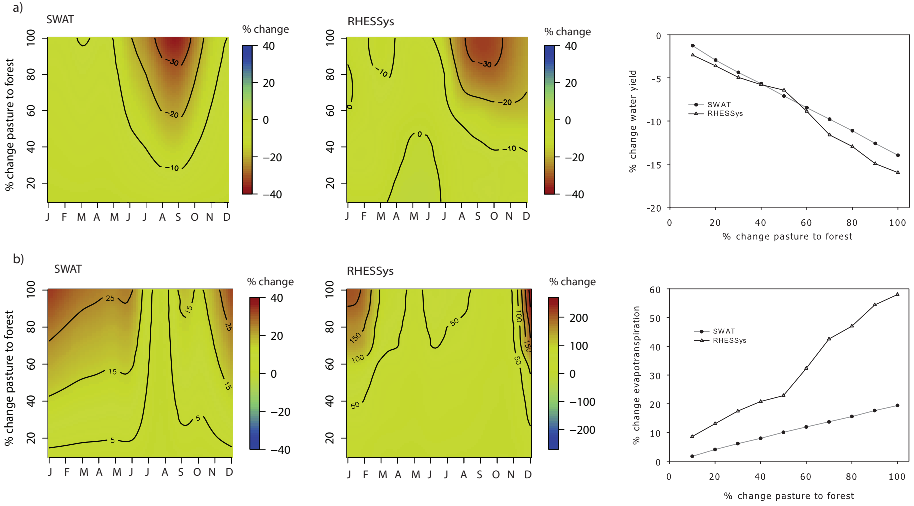

Fig. 9. Relative changes in water yield **(a)** and evapotranspiration **(b)** when pasture is progressively (10 %, 20 % ... 100 %) converted to pine forest in the selected sub-basin. Note that color scales ranges from red (negative) to blue (positive) in the case of stream flow, and vice-versa in the case of evapotranspiration. Smoothed surface and contours were obtained by interpolating results with splines interpolation method.